Numerical Solutions of the Elliptic Differential and the Planetary Motion Equations by Haar Wavelet - Quasilinearization Technique

Rawipa Yangchareonyuanyong[†], **Sanoe Koonprasert**[†,‡,1] **and**
Sekson Sirisubtawee[†,‡]

[†]Department of Mathematics, Faculty of Applied Science, King Mongkut's
University of Technology North Bangkok, Bangkok 10800, Thailand
e-mail : y.rawipa@gmail.com (R.Yangchareonyuanyong)
[‡]Centre of Excellence in Mathematics, CHE, Si Ayutthaya Rd.,
Bangkok 10400, Thailand
e-mail : sanoe.k@sci.kmutnb.ac.th (S.Koonprasert)
sekson.s@sci.kmutnb.ac.th (S.Sirisubtawee)

Abstract : In this article, we apply the Haar-quasilinearization method (HQM) to solve the second order elliptic differential and planetary motion equations to which initial conditions and three types of boundary conditions including Dirichlet, Neumann-Robin, and Dirichlet-Neumann boundary conditions are equipped. By the HQM, both equations can be reduced to the recurrence relations which are linearized differential equations and then applied the Haar-quasilinearization method for solving these equations. Moreover, comparisons of the obtained results for the constructed problems with the exact solutions, HQM solutions, and some numerical solutions obtained using the standard methods are graphically demonstrated. In particular, the absolute errors, the L_2-norm errors and the maximum absolute errors L_∞ among these solutions are computed. As a result, the HQM is considered as the effective and rapidly convergent scheme.

Keywords : Haar wavelet; elliptic differential equation; quasilinearization method; planetary motion equation; wavelet collocation points; Runge-Kutta Fehlberg method.
2010 Mathematics Subject Classification : 65T60; 34B05.

---

[1]Corresponding author.

1   Introduction

In the field of differential equations, the studies of initial value problems (IVPs) and boundary value problems (BVPs) in the ordinary differential equations (ODEs) have attracted the attention of many mathematicians and physicists. Many methods including numerical and perturbation methods have been used to solve such types of problems [1]. Many powerful and efficient methods which can solve both singularity and non-singularity problems have been developed to obtain solutions of the initial and boundary value problems. These methods include the Haar wavelet collocation method (HWCM) [1], the Haar-quasilinearization method, the Laguerre wavelets method, the differential transform method (DTM) [2], the homotopy perturbation method (HPM) [3], the Laplace-variational iteration method (LVIM) [4], the Adomian decomposition method (ADM), and the Chebyshev wavelet collocation method.

One of the popular families of wavelets is Haar wavelet. Due to its simplicity, Haar wavelet has become an effective tool for solving differential equations. In 1997, the Haar wavelet was introduced in a system analysis by Chen and Hsiao [5], who first derived a Haar operational matrix for the integrals of the Haar function vector and provided the applications for the Haar analysis into the dynamic systems. In 2007, Lepik [6] applied the HWCM to differential and integral equations to obtain numerical solutions. In 2008, Bujurke et al. [7] employed the Haar wavelet method to obtain the solutions of nonlinear oscillator equations, stiff systems, and regular Sturm-Liouville problems, etc. In 2010, Islam et al. [8] obtained the numerical solutions of second-order boundary-value problems using the HWCM for the different boundary conditions.

However, the quasilinearization method [9, 10] is a well-known technique to obtain approximate solutions of nonlinear differential equations with rapid convergence. The fundamental of the method of quasilinearization lies in the theory of dynamical programming. Indeed, the quasilinearization technique is a variant version of Newton's method. It can be used to solve for both IVPs and BVPs. Generally, this method is implemented for the problems with convex or concave nonlinearities. The method of quasilinearization has recently been studied and extended extensively. For example, Bellman and Kalaba [10] used the method of quasilinearization as a generalization of the Newton-Raphson method [11] to solve the individual or system of nonlinear ordinary and partial differential equations. Recently, applications of the approach, which can be found in [9], are quite wondrous and easy for obtaining approximate solutions of nonlinear differential equations with finite or infinite delay, integral equations, functional equations, and so on. Hence, the quasilinearization approach is suitable for obtaining solutions of general nonlinear ordinary differential equations.

We introduce the generalized second order differential equation with variable coefficients as

$$\frac{d^2y(x)}{dx^2} = a(x) + b(x)y(x) + c(x)y^2(x) + d(x)y^3(x), \tag{1.1}$$

where the coefficients $a(x)$, $b(x)$, $c(x)$, and $d(x)$ are real-valued functions. In this paper, we let $a(x) = \frac{\varepsilon^2}{2}g_1$, $b(x) = \varepsilon^2 g_2$, $c(x) = \frac{3}{2}\varepsilon^2 g_3$, and $d(x) = 2\varepsilon^2 g_4$ where ε, g_1, g_2, g_3 and g_4 are constants. Then Eq. (1.1) is reduced to

$$\frac{d^2 y(x)}{dx^2} = \varepsilon^2 \left(\frac{g_1}{2} + g_2 y(x) + \frac{3}{2}g_3 y^2(x) + 2g_4 y^3(x) \right), \tag{1.2}$$

Eq. (1.2) is called the second order elliptic differential equation. In particular, we set $\varepsilon = 1$, $g_1 = \lambda$, $g_2 = -1$, $g_3 = \rho$ and $g_4 = 0$ where λ and ρ are constants. Then Eq. (1.2), becomes

$$\frac{d^2 y(x)}{dx^2} = \frac{\lambda}{2} - y(x) + \frac{3}{2}\rho y^2(x), \tag{1.3}$$

which is called the planetary motion equation [12]. The aim of this paper is to construct numerical solutions of the elliptic differential equation (1.2) and the planetary motion equation (1.3) using the Haar wavelet-quasilinearization method with the following various initial and/or boundary conditions.

- Initial conditions : $y(0) = \alpha_1$, $y'(0) = \beta_1$,

- Dirichlet boundary conditions : $y(0) = \alpha_2$, $y(1) = \beta_2$,

- Neumann-Robin boundary conditions : $y'(0) = \omega$, $\alpha_3 y(1) + \beta_3 y'(1) = \gamma$,

- Dirichlet-Neumann boundary conditions : $y(0) = \alpha_4$, $y'(1) = \beta_4$,

where α_i, β_i, $(i = 1, 2, 3, 4)$, ω, and γ are real constants.

2   Haar Wavelets

In this section, we first briefly review the Haar wavelets and its properties which can be found in [13–17]. The Haar wavelet family defined on the interval $[0, 1)$ consists of the following Haar functions:

$$h_1(x) = \begin{cases} 1, & x \in [0, 1), \\ 0, & \text{otherwise,} \end{cases} \tag{2.1}$$

and for $i = 2, 3, \ldots$

$$h_i(x) = \begin{cases} 1, & x \in \left[\frac{k}{m}, \frac{k+0.5}{m}\right), \\ -1, & x \in \left[\frac{k+0.5}{m}, \frac{k+1}{m}\right), \\ 0, & \text{otherwise.} \end{cases} \tag{2.2}$$

where the integer $m = 2^j$, $j = 0, 1, \ldots, J$ indicates the level of the wavelet with the maximal level of resolution J and $k = 0, 1, \ldots, m-1$ is the translation parameter. The index i in Eq. (2.2) is expressed by the intergers m and k as $i = m+k+1$. It is obvious that the minimal value of i is $i = 2$ when $m = 1$, $k = 0$ and the maximal

value of i is $i = 2^{J+1}$ when $m = 2^J$, $k = 2^J - 1$. The Haar wavelet functions satisfy the following properties:

$$\int_0^1 h_i(x)dx = \begin{cases} 1, & \text{if } i = 1, \\ 0, & \text{if } i = 2, 3, \ldots, \end{cases} \tag{2.3}$$

and the orthogonal property for $i, l = 1, 2, \ldots$

$$\int_0^1 h_i(x)h_l(x)dx = \begin{cases} 2^{-j}, & i = l = 2^j + k, \\ 0, & i \neq l. \end{cases} \tag{2.4}$$

Haar wavelet functions construct a very good transform basis which is used to represent any square integrable function $u(x)$ defined on $[0, 1)$, i.e., $\int_0^1 u^2(x)dx < \infty$. Therefore, any function $u(x)$ can be expressed in terms of an infinite sum of the Haar wavelets as follows.

$$u(x) = \sum_{i=1}^{\infty} a_i h_i(x), \quad i = 2^j + k, \quad j \geqslant 0, \quad 0 \leqslant k \leqslant 2^j, \quad x \in [0, 1), \tag{2.5}$$

where the Haar coefficients

$$a_i = 2^j \int_0^1 u(x)h_i(x)dx. \tag{2.6}$$

In general, the series expansion of $u(x)$ involves infinite terms. Practically, the continuous function $u(x)$ can be approximated using the finite sum of the Haar wavelets, that is

$$u(x) \approx u_{2M}(x) := \sum_{i=1}^{2M} a_i h_i(x), \tag{2.7}$$

where $M = 2^J$ and the integral square error is defined as

$$E = \int_0^1 [u(x) - u_{2M}(x)]^2 \, dx. \tag{2.8}$$

The approximation $u_{2M}(x)$ can be written as

$$u_{2M}(x) = \mathbf{a}^T \mathbf{h}, \tag{2.9}$$

where $\mathbf{a}^T = [a_1, a_2, \ldots, a_{2M}]$ is called the coefficient vector and $\mathbf{h} = [h_1(x), h_2(x), \ldots, h_{2M}(x)]^T$ is the Haar function vector.
   Defining the wavelet collocation points x_l as

$$x_l = \frac{l - 0.5}{2M}, \quad l = 1, 2, \ldots, 2M, \tag{2.10}$$

and constructing the Haar wavelet matrix $\mathbf{H}_{2M}$ of order $2M$ in which its columns are the Haar function vectors evaluated at x_l, $l = 1, 2, ..., 2M$. In other words, $\mathbf{H}_{2M}(i, l) = h_i(x_l)$, or the $2M \times 2M$ matrix $\mathbf{H}_{2M}$ is

$$\mathbf{H}_{2M} = \begin{bmatrix} h_1(x_1) & h_1(x_2) & \ldots & h_1(x_{2M}) \\ h_2(x_1) & h_2(x_2) & \ldots & h_2(x_{2M}) \\ \vdots & \vdots & \ddots & \vdots \\ h_{2M}(x_1) & h_{2M}(x_2) & \ldots & h_{2M}(x_{2M}) \end{bmatrix}. \tag{2.11}$$

For example, if $J = 2 \Rightarrow 2M = 2^{J+1} = 8$, then the Haar wavelet matrix of order 8 is

$$\mathbf{H}_8 = \begin{bmatrix} 1 & 1 & 1 & 1 & 1 & 1 & 1 & 1 \\ 1 & 1 & 1 & 1 & -1 & -1 & -1 & -1 \\ 1 & 1 & -1 & -1 & 0 & 0 & 0 & 0 \\ 0 & 0 & 0 & 0 & 1 & 1 & -1 & -1 \\ 1 & -1 & 0 & 0 & 0 & 0 & 0 & 0 \\ 0 & 0 & 1 & -1 & 0 & 0 & 0 & 0 \\ 0 & 0 & 0 & 0 & 1 & -1 & 0 & 0 \\ 0 & 0 & 0 & 0 & 0 & 0 & 1 & -1 \end{bmatrix}. \tag{2.12}$$

In consequence, we have

$$\mathbf{U}_{2M}^T = \mathbf{a}^T \mathbf{H}_{2M}, \tag{2.13}$$

where $\mathbf{U}_{2M}^T = \begin{bmatrix} u_{2M}(x_1), u_{2M}(x_2), \ldots, u_{2M}(x_{2M}) \end{bmatrix}$ is called the discrete form of the continuous function $u(x)$.

Finally, we concisely provide the basic idea of the integrals of the Haar functions $h_i(x)$ of order n denoted by $p_{i,n}(x)$ which can be calculated analytically as follows:

For $i = 1$: the integral of the Haar wavelet, $h_1(x)$ of order n [18] is

$$p_{i,n}(x) = \frac{x^n}{n!}, \quad \text{where} \quad n = 1, 2, \ldots$$

For $i = 2, 3, \ldots$: the integrals of the Haar wavelet, $h_i(x)$, of the first order [19] are

$$p_{i,1}(x) = \int_0^x h_i(s) ds = \begin{cases} x - \frac{k}{m}, & x \in \left[\frac{k}{m}, \frac{k+0.5}{m} \right), \\ \frac{k+1}{m} - x, & x \in \left[\frac{k+0.5}{m}, \frac{k+1}{m} \right), \\ 0, & \text{otherwise}, \end{cases} \tag{2.14}$$

and the integrals of the Haar wavelet, $h_i(x)$, of order n are given by

$$p_{i,n}(x) = \int_0^x p_{i,n-1}(s) ds, \quad n = 2, 3, \ldots \tag{2.15}$$

$$= \frac{1}{n!} \begin{cases} \left(x - \frac{k}{m} \right)^n, & x \in \left[\frac{k}{m}, \frac{k+0.5}{m} \right), \\ \left(x - \frac{k}{m} \right)^n - 2 \left(x - \frac{k+0.5}{m} \right)^n, & x \in \left[\frac{k+0.5}{m}, \frac{k+1}{m} \right), \\ \left(x - \frac{k}{m} \right)^n - 2 \left(x - \frac{k+0.5}{m} \right)^n + \left(x - \frac{k+1}{m} \right)^n, & x \in \left[\frac{k+1}{m}, 1 \right), \\ 0, & \text{otherwise}. \end{cases}$$

Then we define the $2M$ operational matric of integrations $\mathbf{P}_n$ and its element is computed using the relation $\mathbf{P}_n(i,l) = p_{i,n}(x_l)$, where x_l is defined in Eq. (2.10). For example, if $J = 2 \Rightarrow 2M = 8$ and $n = 1$, then from Eq. (2.14), the Haar wavelet integral matrix of the first order as

$$
\mathbf{P}_1 = \frac{1}{16}
\begin{bmatrix}
1 & 3 & 5 & 7 & 9 & 11 & 13 & 15 \\
1 & 3 & 5 & 7 & 7 & 5 & 3 & 1 \\
1 & 3 & 3 & 1 & 0 & 0 & 0 & 0 \\
0 & 0 & 0 & 0 & 1 & 3 & 3 & 1 \\
1 & 1 & 0 & 0 & 0 & 0 & 0 & 0 \\
0 & 0 & 1 & 1 & 0 & 0 & 0 & 0 \\
0 & 0 & 0 & 0 & 1 & 1 & 0 & 0 \\
0 & 0 & 0 & 0 & 0 & 0 & 1 & 1
\end{bmatrix},
\tag{2.16}
$$

and when $n = 2$, the Haar wavelet integral matrix of order 2 is computed by using Eq. (2.16) as

$$
\mathbf{P}_2 = \frac{1}{512}
\begin{bmatrix}
1 & 9 & 25 & 49 & 81 & 121 & 169 & 225 \\
1 & 9 & 25 & 49 & 79 & 103 & 119 & 127 \\
1 & 9 & 23 & 31 & 32 & 32 & 32 & 32 \\
0 & 0 & 0 & 0 & 1 & 9 & 23 & 31 \\
1 & 7 & 8 & 8 & 8 & 8 & 8 & 8 \\
0 & 0 & 1 & 7 & 8 & 8 & 8 & 8 \\
0 & 0 & 0 & 0 & 1 & 7 & 8 & 8 \\
0 & 0 & 0 & 0 & 0 & 0 & 1 & 7
\end{bmatrix}.
\tag{2.17}
$$

2.1   Haar-quasilinearization method

Consider the nonlinear second order differential equation of the form

$$
y''(x) = f(y(x), x).
\tag{2.18}
$$

where f is a function that depends on a function $y(x)$ and x. Applying the Taylor series expansion for $f(y(x), x)$ about the initial function $y_0(x)$, the function f can be then expressed around the function $y_0(x)$ as

$$
y''(x) = f(y_0(x), x) + (y(x) - y_0(x)) f_y(y_0(x), x)
$$
$$
+ \frac{1}{2!} (y(x) - y_0(x))^2 f_{yy}(y_0(x), x) + \dots
\tag{2.19}
$$

Ignoring the second and higher order terms of Eq. (2.19), we get

$$
y''(x) = f(y_0(x), x) + (y(x) - y_0(x)) f_y(y_0(x), x),
\tag{2.20}
$$

where $y_0(x)$ is given. In procedure of the quasilinearization technique to Eq. (2.20), we first obtain the recursive formula for $y_1(x)$ by replacing $y(x)$ in Eq. (2.20) with $y_1(x)$ as follows.

$$
y_1''(x) = f(y_0(x), x) + (y_1(x) - y_0(x)) f_y(y_0(x), x),
\tag{2.21}
$$

where $y_1''(x)$ can be approximated by Haar wavelet, $y_1''(x) = \sum_{i=1}^{2M} a_i^{(1)} h_i(x)$.

By the Haar wavelet method, it obtains $y_1(x)$ from solving Eq. (2.21). Again, substituting $y(x)$ in Eq. (2.20) with $y_2(x)$ and replacing $y_0(x)$ in the equation with $y_1(x)$, we then obtain the new recursive formula as

$$y_2''(x) = f(y_1(x), x) + (y_2(x) - y_1(x)) f_y(y_1(x), x), \tag{2.22}$$

where the function $y_2''(x) = \sum_{i=1}^{2M} a_i^{(2)} h_i(x)$.

We keep continuing the same procedure for obtaining the higher accurate recursive relations, which are based on the Haar-quasilinearization technique. The general form of the recursive scheme is of the form

$$y_{r+1}''(x) = f(y_r(x), x) + (y_{r+1}(x) - y_r(x)) f_y(y_r(x), x), \tag{2.23}$$

where the function $y_{r+1}''(x) = \sum_{i=1}^{2M} a_i^{(r+1)} h_i(x)$, $r = 0, 1, 2, \ldots$ and $y_r(x)$ is a known function.

2.1.1 Initial conditions

Given the initial conditions: $y_{r+1}(0) = \alpha_1$ and $y_{r+1}'(0) = \beta_1$ to Eq. (2.18). Integrating $y_{r+1}''(x) = \sum_{i=1}^{2M} a_i h_i(x)$ from 0 to x and using the initial condition $y_{r+1}'(0) = \beta_1$, we obtain

$$y_{r+1}'(x) = y_{r+1}'(0) + \sum_{i=1}^{2M} a_i p_{i,1}(x) = \beta_1 + \sum_{i=1}^{2M} a_i p_{i,1}(x), \tag{2.24}$$

where $p_{i,1}(x)$ is defined in Eq. (2.14). Again integrating Eq. (2.24) and then using the initial condition $y_{r+1}(0) = \alpha_1$, we have

$$y_{r+1}(x) = y_{r+1}(0) + \beta_1 x + \sum_{i=1}^{2M} a_i p_{i,2}(x) = \alpha_1 + \beta_1 x + \sum_{i=1}^{2M} a_i p_{i,2}(x), \tag{2.25}$$

where $p_{i,2}(x)$ is expressed in Eq. (2.16).

2.1.2 Dirichlet boundary conditions

Given the Dirichlet boundary conditions: $y_{r+1}(0) = \alpha_2$ and $y_{r+1}(1) = \beta_2$ to Eq. (2.18). From Eq. (2.24), we have

$$y_{r+1}'(x) = y_{r+1}'(0) + \sum_{i=1}^{2M} a_i p_{i,1}(x), \tag{2.26}$$

where $y'_{r+1}(0)$ will be determined later. Integrating Eq. (2.26) and then using the Dirichlet boundary condition $y_{r+1}(0) = \alpha_2$, we have

$$y_{r+1}(x) = \alpha_2 + xy'_{r+1}(0) + \sum_{i=1}^{2M} a_i p_{i,2}(x). \qquad (2.27)$$

By substituting $x = 1$ into Eq. (2.27) and applying the Dirichlet boundary condition $y_{r+1}(1) = \beta_2$, the unknown term $y'_{r+1}(0)$ in Eq. (2.27) can be calculated as

$$y'_{r+1}(0) = \beta_2 - \alpha_2 - \sum_{i=1}^{2M} a_i p_{i,2}(1). \qquad (2.28)$$

When we replace the obtained value of $y'_{r+1}(0)$ in Eq. (2.27), then we eventually obtain

$$y_{r+1}(x) = \alpha_2 + x(\beta_2 - \alpha_2) + \sum_{i=1}^{2M} a_i (p_{i,2}(x) - xp_{i,2}(1)). \qquad (2.29)$$

2.1.3   Neumann-Robin boundary conditions

Given the Neumann-Robin boundary conditions: $y'_{r+1}(0) = \omega$ and $\alpha_3 y_{r+1}(1) + \beta_3 y'_{r+1}(1) = \gamma$ to Eq. (2.18). Applying the Neumann-Robin boundary condition $y'_{r+1}(0) = \omega$ to Eq. (2.26), we then have

$$y'_{r+1}(x) = \omega + \sum_{i=1}^{2M} a_i p_{i,1}(x). \qquad (2.30)$$

Integrating Eq. (2.30) with respect to x, we get

$$y_{r+1}(x) = y_{r+1}(0) + x\omega + \sum_{i=1}^{2M} a_i p_{i,2}(x). \qquad (2.31)$$

Substituting $x = 1$ into Eqs. (2.30) and (2.31), we obtain

$$y'_{r+1}(1) = \omega + \sum_{i=1}^{2M} a_i p_{i,1}(1), \qquad (2.32)$$

$$y_{r+1}(1) = y_{r+1}(0) + \omega + \sum_{i=1}^{2M} a_i p_{i,2}(1), \qquad (2.33)$$

respectively. From the property (2.3), we have that

$$\sum_{i=1}^{2M} a_i p_{i,1}(1) = a_1 \int_0^1 h_1(x)dx + a_2 \int_0^1 h_2(x)dx + \cdots + a_{2M} \int_0^1 h_{2M}(x)dx = a_1. \qquad (2.34)$$

Applying Eqs. (2.32)-(2.34) to the rest boundary condition, we have

$$\alpha_3 \left[y_{r+1}(0) + \omega + \sum_{i=1}^{2M} a_i p_{i,2}(1) \right] + \beta_3 \left[\omega + a_1 \right] = \gamma,$$

$$y_{r+1}(0) = \frac{\gamma}{\alpha_3} - \frac{\beta_3}{\alpha_3} \left[\omega + a_1 \right] - \omega - \sum_{i=1}^{2M} a_i p_{i,2}(1). \qquad (2.35)$$

Substituting $y_{r+1}(0)$ in Eq. (2.35) into Eq. (2.31), the Haar-quasilinearization solution of Eq. (2.18) equipped with the given Neumann-Robin boundary conditions is

$$y_{r+1}(x) = \frac{\gamma}{\alpha_3} - \frac{\beta_3}{\alpha_3} \left[\omega + a_1 \right] + (x-1)\omega + \sum_{i=1}^{2M} a_i \left(p_{i,2}(x) - p_{i,2}(1) \right). \qquad (2.36)$$

2.1.4 Dirichlet-Neumann boundary conditions

Given the Dirichlet-Neumann boundary conditions: $y_{r+1}(0) = \alpha_4$ and $y'_{r+1}(1) = \beta_4$ to Eq. (2.18). Integrating $y''_{r+1}(x) = \sum_{i=1}^{2M} a_i h_i(x)$ with respect to x with the lower limit $x = 0$ and the upper limit $x = 1$ and then using the condition $y'_{r+1}(1) = \beta_4$ and Eq. (2.34), we get

$$y'_{r+1}(0) = y'_{r+1}(1) - \sum_{i=1}^{2M} a_i \int_0^1 h_i(x)dx = \beta_4 - a_1. \qquad (2.37)$$

Hence, we substitute the above result into Eq. (2.26) to obtain

$$y'_{r+1}(x) = \beta_4 - a_1 + \sum_{i=1}^{2M} a_i p_{i,1}(x). \qquad (2.38)$$

Finally, we integrate Eq. (2.38) with respect to x and then use the rest boundary condition $y_{r+1}(0) = \alpha_4$ to obtain the desired relation as follows:

$$y_{r+1}(x) = \alpha_4 + (\beta_4 - a_1) x + \sum_{i=1}^{2M} a_i p_{i,2}(x). \qquad (2.39)$$

3 Numerical Results and Discussion

Examining the accuracy and applicability of the Haar-quasilinearization method (HQM), we will firstly use the Haar-quasilinearization method to numerically solve the second order elliptic differential equation (1.2) that equipped with some kinds of the following conditions: the initial conditions, Dirichlet boundary conditions,

Neumann-Robin boundary conditions, and Dirichlet-Neumann boundary conditions. Secondly, this method will be used to solve the initial value problem of the planetary motion equation (1.3). Our obtained numerical solutions of the considering problems will be compared with their exact solutions for some types of the error. The error types are used in our simulations are the absolute error, the L_2-norm of the error and the L_∞-norm of the error, which are defined as [20]

$$\text{Abs. error} = |y(x) - y_h(x)|, \tag{3.1}$$

$$L_2 = \left(\sum_{l=1}^{2M} |y(x_l) - y_h(x_l)|^2 \right)^{\frac{1}{2}}, \tag{3.2}$$

$$L_\infty = \max_{x \in [0,1]} |y(x) - y_h(x)|, \tag{3.3}$$

respectively. The solutions $y(x)$ and $y_h(x)$ in Eqs. (3.1)-(3.3) represent an exact solution and a numerical solution. All of the HQM computations will be performed using the HQM coding that is generated in the Maple program.

3.1 The second order elliptic differential equation

Problem 1: Consider the following initial value problem

$$\frac{d^2 y(x)}{dx^2} = -1.3025 y(x) + 0.605 y^3(x),$$
$$y(0) = 0.819, \quad y'(0) = 0.513. \tag{3.4}$$

The differential equation in Eq. (3.4) is obtained by substituting $\varepsilon = 1$, $g_1 = g_3 = 0$, $g_2 = -(1 + \kappa^2)$, $g_4 = \kappa^2$ where $\kappa = 0.55$ into Eq. (1.2). The exact solution of this problem is $y(x) = \mathbf{sn}\left(x + 1, \frac{11}{20}\right)$ with the modulus $k = \frac{11}{20}$, which $\mathbf{sn}(u, k)$ is the Jacobi elliptic sine function with modulus $0 \leqslant k \leqslant 1$.

The Haar-quasilinearization method (HQM) with the maximal level of resolution $J = 3$ and the Runge-Kutta Fehlberg method (RKF) which is the default one for solving initial value problems in the Maple program package are used to solve Eq. (3.4) for numerical solutions. The exact solution $y(x)$ and the numerical solutions ($y_{RKF}(x)$ and $y_{HQM}(x)$) are evaluated at some collocation points in [0, 1] which their numerical values are shown in Table 1. In addition, Table 1 also shows the absolute errors between the exact values and the numerical values generated using the two methods. The graphical representations of these solutions are plotted in Fig. 1.

Next, we investigate the effective maximal values of resolution J used in the HQM for improving the obtained numerical solutions for Eq. (3.4). The graphs of the absolute errors $|y(x) - y_{RKF}(x)|$ and $|y(x) - y_{HQM}(x)|$ calculated at the maximal levels of resolution for $J = 3, 4, 5, 6$ can be depicted in the Fig. 2.

Table 1: Comparisons of the solutions $y(x)$(exact), $y_{RKF}(x)$ and $y_{HQM}(x)(J = 3)$ in Eq. (3.4) in the sense of the absolute error.

x	Exact	RKF	HQM	$|y(x) - y_{RKF}(x)|$	$|y(x) - y_{HQM}(x)|$
1/32	0.83424570	0.83424570	0.83424541	2.0766e-11	2.8895e-7
5/32	0.88974212	0.88974230	0.88974134	1.7684e-7	7.8430e-7
9/32	0.93379771	0.93379775	0.93379749	4.3859e-8	2.1710e-7
13/32	0.96654869	0.96654876	0.96654936	6.1556e-8	6.6471e-7
17/32	0.98816247	0.98816255	0.98816375	7.7920e-8	1.2799e-6
21/32	0.99878152	0.99878157	0.99878275	5.9023e-8	1.2370e-6
25/32	0.99848537	0.99848543	0.99848571	5.6831e-8	3.3854e-7
29/32	0.98727173	0.98727179	0.98727032	5.8937e-8	1.4166e-6
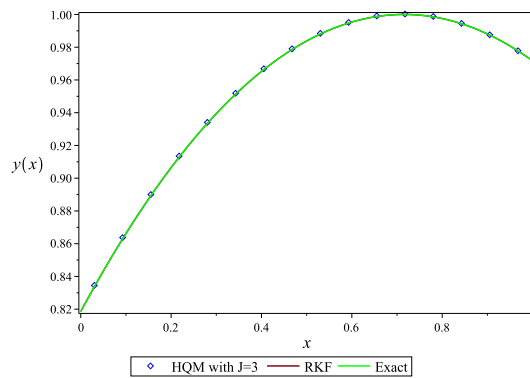
Figure 1: Graphs of $y(x)$, $y_{RKF}(x)$ and $y_{HQM}(x)(J = 3)$ for Eq. (3.4).

Problem 2: Consider the following boundary value problem

$$\frac{d^2 y(x)}{dx^2} = -1.0729y(x) + 2y^3(x),$$
$$y(0) = 0.0424, \quad y(1) = -0.3596. \tag{3.5}$$

The differential equation in Eq. (3.5) is obtained by substituting $\varepsilon = 1$, $g_1 = g_3 = 0$, $g_2 = -(1 + \kappa^2)$, $g_4 = 1$ where $\kappa = 0.27$ into Eq. (1.2). The exact solution of this problem is given by $y(x) = 0.503\mathbf{sn}\,(0.905x + 3.354, 0.556)$ for modulus $k = 0.556$.

　　The Haar-quasilinearization method (HQM) with the maximal levels of resolution $J = 4$ and the finite difference technique with Richardson extrapolation method (REM) which is the default one for solving boundary value problems in the Maple program package are used to solve Eq. (3.5) for numerical solutions.
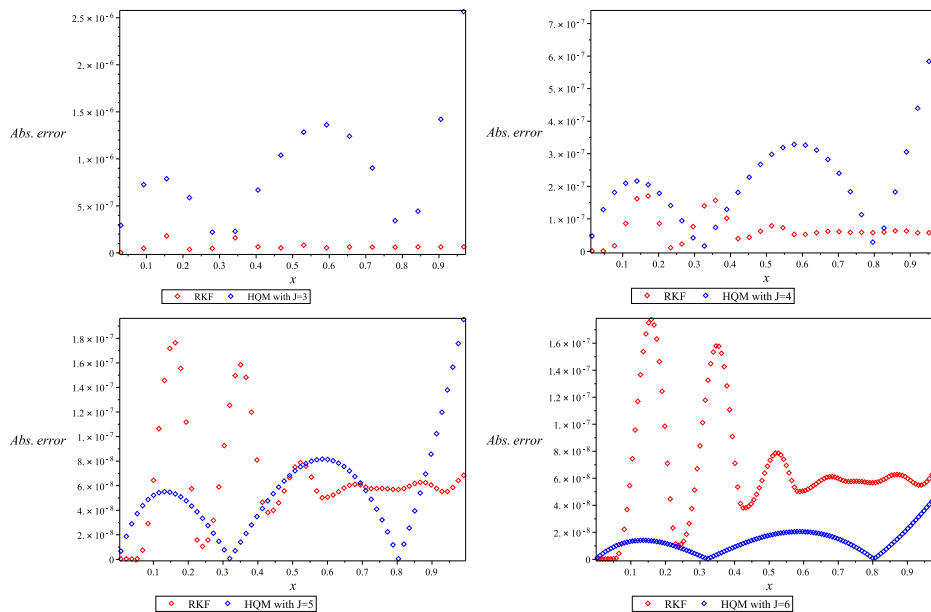
Figure 2: Graphs of RKF=$|y(x) - y_{RKF}(x)|$ and HQM=$|y(x) - y_{HQM}(x)|$ with $J = 3$, 4, 5, 6 for Eq. (3.4).

The exact solution $y(x)$, the numerical solutions $y_{REM}(x)$ and $y_{HQM}(x)$ are evaluated at some collocation points in $[0, 1]$ which their numerical values are shown in Table 2. In addition, Table 2 also shows the absolute errors between the exact values and the numerical values generated using the two methods at such selected points.

Next, we investigate the effect of values of the resolution J used in the HQM for improving the numerical solutions for Eq. (3.5). The graphs of the absolute errors $|y(x) - y_{REM}(x)|$ and $|y(x) - y_{HQM}(x)|$ calculated at the wavelet collocation points for the maximal levels of resolution $J = 3$, 4, 5, 6 can be plotted in the Fig. 3.

Table 2: Comparisons of $y(x)$ (exact) and the numerical results $y_{RKF}(x)$, $y_{HQM}(x)(J=4)$ in Eq. (3.5) in the sense of the absolute error.

x	Exact	REM	HQM	$|y(x) - y_{REM}(x)|$	$|y(x) - y_{HQM}(x)|$
1/64	3.53023e-2	3.53025e-2	3.53025e-2	1.3318e-7	1.0296e-7
9/64	-2.15855e-2	-2.15855e-2	-2.15846e-2	6.7180e-8	9.4754e-7
17/64	-7.81134e-2	-7.81133e-2	-7.81117e-2	9.5449e-8	1.7272e-6
25/64	-0.133352	-0.133352	-0.13335	1.1507e-7	2.3065e-6
33/64	-0.18644	-0.18644	-0.18644	1.2416e-7	2.5781e-6
41/64	-0.236613	-0.23661	-0.23661	1.1000e-7	2.4723e-6
49/64	-0.28325	-0.28325	-0.28324	7.7895e-8	1.9633e-6
57/64	-0.32585	-0.325854	-0.325853	3.7551e-8	1.0657e-6
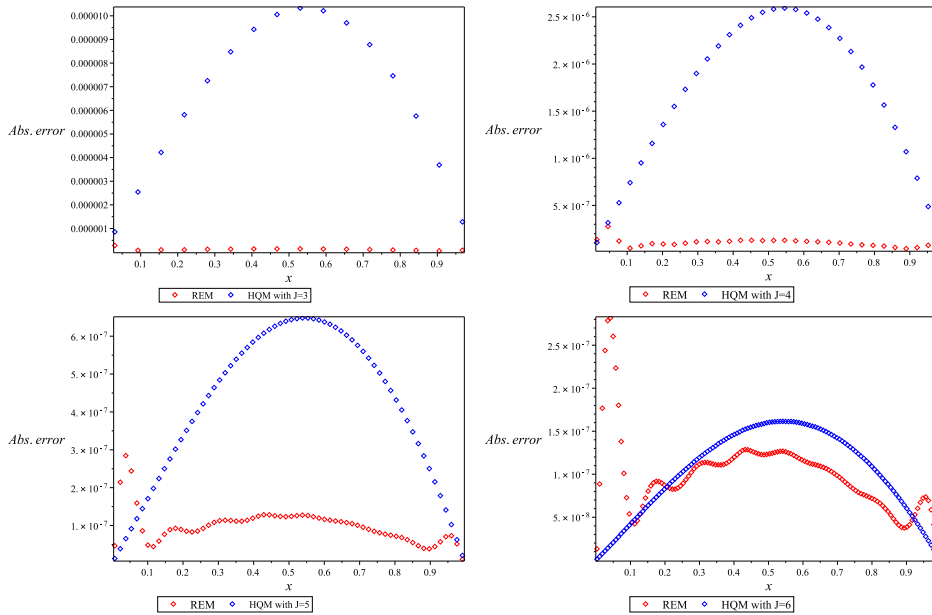
Figure 3: Graphs of REM=$|y(x) - y_{REM}(x)|$ and HQM=$|y(x) - y_{HQM}(x)|$ with $J = 3, 4, 5, 6$ for Eq. (3.5).

Problem 3: Consider the following boundary value problem

$$\frac{d^2 y(x)}{dx^2} = -0.9688 y(x) + 0.0312 y^3(x),$$

$$y'(0) = 0.52625, \quad 2y(1) + y'(1) = 1.4715. \tag{3.6}$$

The differential equation in Eq. (3.6) is obtained by substituting $\varepsilon = 1$, $g_1 = g_3 = 0$, $g_2 = \frac{\kappa^2 - 2}{2}$, $g_4 = \frac{\kappa^2}{4}$ where $\kappa = 0.25$ into Eq. (1.2). The exact solution is $y(x) = \mathbf{sn}\left(\frac{\sqrt{61}}{8}x + 1, \frac{\sqrt{61}}{61}\right)$ at the modulus $k = \frac{\sqrt{61}}{61}$.

The Haar-quasilinearization method (HQM) with the maximal levels of resolution $J = 5$ and the finite difference technique with Richardson extrapolation method (REM) are used to solve Eq. (3.6) for numerical solutions. The exact solution $y(x)$, the numerical solutions $y_{REM}(x)$ and $y_{HQM}(x)$ are evaluated at some collocation points in $[0, 1]$ which their numerical values are plotted in Fig. 4.
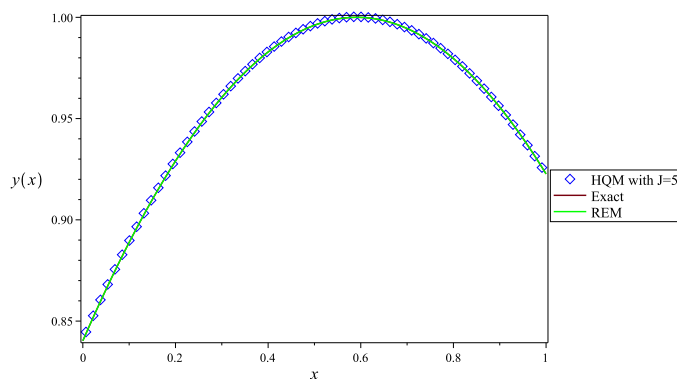
Figure 4: Graphs of the exact solution and the numerical solutions $(y_{RKF}(x)$ and $y_{HQM}(x)(J = 5))$ for Eq. (3.6).

The improvement of the obtained numerical solutions for Eq. (3.6) is studied by the effective maximal values of resolution J. In other words, the L_2-norm and the L_∞-norm of errors calculated at the wavelet collocation points in $[0, 1]$ for $J = 2, 3, 4, 5, 6$ are reported in Table 3. As a result, the higher values of resolution J promisingly provide the better numerical solutions compared with the lower values of resolution J.

Table 3: L_2 and L_∞ of the errors obtained using the HQM with $J = 2, 3, 4, 5, 6$ for Eq.(3.6).

J	2	3	4	5	6
$2M$	8	16	32	64	128
L_2	4.872e-3	1.72e-3	6.077e-4	2.148e-4	7.594e-5
L_∞	2.16e-3	5.447e-4	1.368e-4	3.426e-5	8.574e-6

Problem 4: Consider the following boundary value problem

$$\frac{d^2y(x)}{dx^2} = -1.9025y(x) + 2y^3(x),$$

$$y(0) = 0.2129, \quad y'(1) = -0.2734. \tag{3.7}$$

The differential equation in Eq. (3.7) is attained by replacing $\varepsilon = 1$, $g_1 = g_3 = 0$, $g_2 = -(1 + \kappa^2)$, $g_4 = 1$ where $\kappa = 0.95$ into Eq. (1.2). The exact solution of this problem is $y(x) = 0.2151\mathbf{sn}(1.3624x + 1.4341, 0.1579)$ with the modulus $k = 0.1579$. For this problem, the numerical results generated using the HQM are only compared with $y(x)$. The absolute errors $|y(x) - y_{HQM}(x)|$ are computed at the collocation points for the maximal levels of resolution $J = 3$, 4, 5, 6 in the HQM. Their graphs are shown in Fig. 5. We can observe from Fig. 5 that the resolution $J = 6$ for the HQM gives the best numerical solution for the problem.
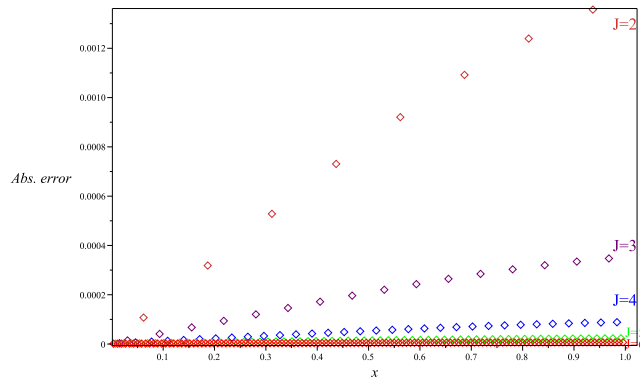
Figure 5: Comparison of the absolute errors between $y(x)$ and $y_{HQM}(x)$ with the maximal levels of resolution $J = 2$, 3, 4, 5, 6 for Eq. (3.7).

Next, we study how to improve the obtained numerical solutions for Eq. (3.7) by increasing the maximal values of resolution J in the HQM. This can be done by computing the L_2-norm and the L_∞-norm errors calculated at the wavelet collocation points in $[0, 1]$ for $J = 2$, 3, 4, 5, 6. These errors are numerically reported in Table 4. As a result, using the higher values of J in the HQM quite gaurantees that the better numerical solutions of the problem are obtained.

Problem 5: Consider the following boundary value problem

$$\frac{d^2y(x)}{dx^2} = 1.125e^x - 2.930625y(x) + 3.375xy^2 + 4.5x^2y^3(x),$$

$$y(0) = 0.8186, \quad y(1) = 0.7813. \tag{3.8}$$

The differential equation in Eq. (3.8) is attained by replacing $\varepsilon = 1.5$, $g_1 = e^x$, $g_2 = -(1 + \kappa^2)$, $g_3 = x$, $g_4 = x^2$ where $\kappa = 0.55$ into Eq. (1.2). This problem is

Table 4: L_2 and L_∞ errors obtained using the HQM with $J = 2$, 3, 4, 5, 6 for Eq.(3.7).

J	2	3	4	5	6
$2M$	8	16	32	64	128
L_2	2.51497e-3	8.9169e-4	3.1549e-4	1.1156e-4	3.9445e-5
L_∞	1.3554e-3	3.4575e-4	8.7196e-5	2.1887e-5	5.4824e-6

quite special and different from the previous problems because g_1, g_3, and g_4 are functions of x, not constants. Since it is hard to find the exact solution of this problem, then numerical solutions obtained using the REM and HQM with $J = 5$ are only computed at the selected collocation points. These numerical solutions of this problem are portrayed in Fig. 6.
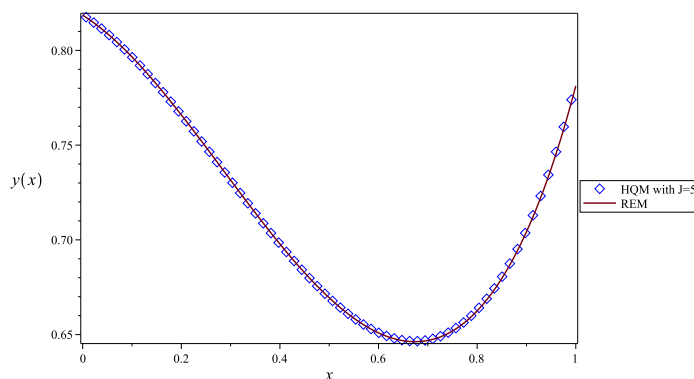
Figure 6: Numerical solutions obtained using the $y_{REM}(x)$ and $y_{HQM}(x)$ with $J = 5$ for Eq. (3.8).

3.2   The planetary motion equation

Problem 1: Consider the following initial value problem

$$\frac{d^2y(x)}{dx^2} + y(x) = 0.0435 + \frac{3}{2}y^2(x),$$

$$y(0) = 0.895, \quad y'(0) = 0. \tag{3.9}$$

The differential equation in Eq. (3.9) is obtained by substituting $\lambda = 0.087$, $\rho = 1$ into the planetary motion equation (1.3). The exact solution of this problem is $y(x) = 0.1511 + 0.7439\mathbf{nc}^2(0.4851x, 0.2096)$ with modulus $k = 0.2096$, which

$\mathbf{nc}(u, k)$ is a reciprocal of the Jacobi elliptic cosine function.

The Haar-quasilinearization method (HQM) with the maximal levels of resolution $J = 5$ and the Runge-Kutta Fehlberg method (RKF) are used to solve Eq. (3.9) for numerical solutions. The exact solution $y(x)$, $y_{RKF}(x)$ and $y_{HQM}(x)$ are evaluated at some wavelet collocation points in $[0, 1]$ which their numerical values are shown in Table 5. Moreover, Table 5 also shows the absolute errors between the exact values and the numerical values generated using the two methods at such selected points. The graphical representations of these solutions are plotted in Fig. 7.

Table 5: Comparisons of the numerical results ($y(x)$, $y_{RKF}(x)$ and $y_{HQM}(x)(J = 5)$) in Eq. (3.4) in the sense of the absolute error.

x	Exact	RKF	HQM	$|y(x) - y_{RKF}(x)|$	$|y(x) - y_{HQM}(x)|$
1/128	0.8950107	0.8950107	0.8950107	6.8830e-10	1.1461e-9
11/128	0.8962940	0.8962939	0.8962939	1.2862e-7	1.0401e-7
21/128	0.8997304	0.8997288	0.8997288	1.6675e-6	1.5833e-6
31/128	0.9053588	0.9053508	0.9053510	7.9644e-6	7.7796e-6
41/128	0.9132434	0.9132188	0.9132191	2.4623e-5	2.4293e-5
51/128	0.9234757	0.9234159	0.9234164	5.9785e-5	5.9268e-5
61/128	0.9361759	0.9360514	0.9360522	1.2455e-4	1.2379e-4
71/128	0.9514972	0.9512637	0.9512647	2.3348e-4	2.3242e-4
81/128	0.9696284	0.9692230	0.9692245	4.0540e-4	4.0395e-4
91/128	0.9908004	0.9901361	0.9901380	6.6429e-4	6.6237e-4
101/128	1.0152915	1.0142508	1.0142533	1.0406e-3	1.0382e-3
111/128	1.0434364	1.0418633	1.0418665	1.5731e-3	1.5699e-3
121/128	1.0756363	1.0733257	1.0733297	2.3106e-3	2.3066e-3

4   Conclusions

In this paper, we have proposed the quasilinearization technique including the Haar wavelet method to numerically solve the second order elliptic differential and planetary motion equations that equipped with one of the following conditions: initial conditions, Dirichlet boundary conditions, Neumann-Robin boundary conditions, and Dirichlet-Neumann boundary conditions. Using the HQM, the numerical results of each problem have been compared with their exact solutions (if any) and the numerical solutions obtained by the other default methods in the
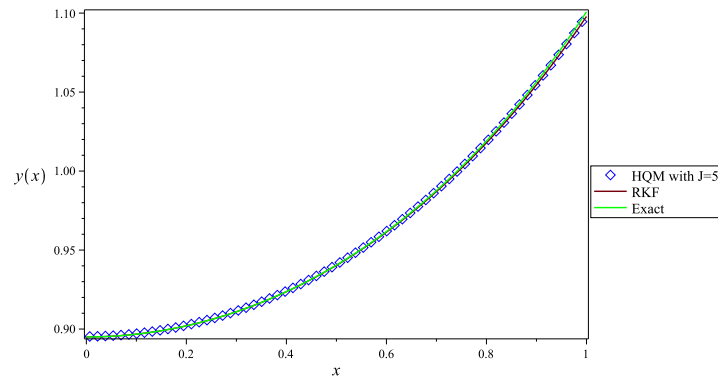
Figure 7: Graphs of $y(x)$, $y_{RKF}(x)$ and $y_{HQM}(x)$ with $J = 5$ for Eq. (3.9).

Maple program package. Certain kinds of the errors such as the absolute error, the L_2-norm of error and the L_∞-norm of error have been calculated using these solutions. Comparisons among the resulting solutions and the errors have been graphically shown to confirm that the HQM yields the highly accurate and rapidly convergent results depending upon the resolution level. The Haar wavelet quasi-linearization method could be effectively applied to solve a wide range of nonlinear differential equations including the case of variable coefficients.

References

[1] S. Shiralashetti, A. Deshi, P.M. Desai, Haar wavelet collocation method for the numerical solution of singular initial value problems, Ain Shams Engineering Journal 7 (2) (2016) 663–670.

[2] Z.M. Odibat, Differential transform method for solving Volterra integral equation with separable kernels, Mathematical and Computer Modelling 48 (7-8) (2008) 1144–1149.

[3] J.-H. He, An elementary introduction to the homotopy perturbation method, Computers & Mathematics with Applications 57 (3) (2009) 410–412.

[4] P. Goswami, R.T. Alqahtani, On the solution of local fractional differential equations using local fractional Laplace variational iteration method, Mathematical Problems in Engineering 2016 (2016).

[5] C. Chen, C. Hsiao, Haar wavelet method for solving lumped and distributed-parameter systems, IEE Proceedings-Control Theory and Applications 144 (1) (1997) 87–94.

[6] Ü. Lepik, Application of the Haar wavelet transform to solving integral and differential equations, in Proceedings of the Estonian Academy of Sciences, Physics, Mathematics 56 (2007).

[7] N. Bujurke, C. Salimath, S. Shiralashetti, Numerical solution of stiff systems from nonlinear dynamics using single-term Haar wavelet series, Nonlinear Dynamics 51 (4) (2008) 595–605.

[8] S-U. Islam, I. Aziz, B. Šarler, The numerical solution of second-order boundary-value problems by collocation method with the Haar wavelets, Mathematical and Computer Modelling 52 (9-10) (2010) 1577–1590.

[9] C. Yakar, Quasilinearization Method in Causal Differential Equations with Initial Time Difference, Commun. Fac. Sci. Univ. Ank. Series A 1 (2014) 2014.

[10] R.E. Bellman, R.E. Kalaba, Quasilinearization and nonlinear boundary-value problems, Rand Corporation, 1965.

[11] S.D. Conte, C.De Boor, Elementary numerical analysis: an algorithmic approach, SIAM 78 (2017).

[12] S. Salas, H. Castillo, R. Restrepo, The Jacobi elliptic functions and their applications in the advance of mercury's perihelion, Revista mexicana de física, Sociedad Mexicana de Física 61 (5) (2015) 392–399.

[13] C.-H. Hsiao, W.-J. Wang, Haar wavelet approach to nonlinear stiff systems, Mathematics and Computers in Simulation 57 (6) (2001) 347–353,

[14] C. Hsiao, Haar wavelet approach to linear stiff systems, Mathematics and Computers in Simulation 64 (5) (2004) 561–567.

[15] Ü. Lepik, Numerical solution of differential equations using Haar wavelets, Mathematics and Computers in Simulation 68 (2) (2005) 127–143.

[16] Ü. Lepik, Numerical solution of evolution equations by the Haar wavelet method, Applied Mathematics and Computation 185 (1) (2007) 695–704.

[17] M.ur Rehman, R.A. Khan, A numerical method for solving boundary value problems for fractional differential equations, Applied Mathematical Modelling 36 (3) (2012) 894–907.

[18] Q. Dai, Q. Cao, Parametric instability analysis of truncated conical shells using the Haar wavelet method, Mechanical Systems and Signal Processing 105 (2018) 200–213.

[19] J. Majak, M. Pohlak, K. Karjust, M. Eerme, J. Kurnitski, B. Shvartsman, New higher order Haar wavelet method: application to FGM structures, Composite Structures 201 (2018) 72–78.

[20] R. Singh, H. Garg, V. Guleria, Haar wavelet collocation method for Lane–Emden equations with Dirichlet, Neumann and Neumann–Robin boundary conditions, Journal of Computational and Applied Mathematics 346 (2019) 150–161.